Journal of Petroleum Research and Studies

journal homepage: https://jprs.gov.iq/index.php/jprs/

Print ISSN 2220-5381, Online ISSN 2710-1096

# Synthesis and Performance of $Mo_2C$-Modified HY Zeolite Catalysts for Naphtha Reforming

**Ban A. Altabbakh[1]*, Aysar T. Jarullah[2], Ahmed N. Ahmed[2]**
[1]Petroleum Research and Development Center, Ministry of Oil, Baghdad, Iraq.
[2]Department of Chemical Engineering, College of Engineering, Tikrit University, Salahaddin, Iraq.
*Corresponding Author E-mail: dr.bana_altabbakh@prdc.oil.gov.iq

**Article Info**

**Received** 11/01/2024
**Revised** 12/04/2026
**Accepted** 12/04/2026
**Published** 21/06/2026

DOI:
http://doi.org/10.52716/jprs.v16i2.912

## Abstract

$Mo_2C$-modified HY zeolite catalysts were developed to enhance dehydrogenation and isomerization reactions in naphtha catalytic reforming. Two composite systems, Pt–Ti/HY and $Mo_2C$–Pt/CeY, were synthesized and characterized using XRD, BET, and FTIR.techniques. Catalytic performance was evaluated in a pilot reforming unit at temperatures of 480–520 °C, pressures of 10–15 bar, LHSV of 2 $h^{-1}$, and $H_2$/HC ratio of 4.

Results indicate that titanium incorporation improves metal–acid balance and promotes hydrogenation–dehydrogenation functionality through the formation of tetrahedrally coordinated Ti species. Among the tested catalysts, Pt–Ti/HY exhibited superior performance, achieving a research octane number of 86.2 and aromatics yield of 27.2 wt% at 520 °C and 15 bar. These findings demonstrate that metal modification of HY zeolite significantly enhances catalytic activity and selectivity in naphtha reforming.

***Keywords:*** Catalytic Reforming, Carbide catalyst, zeolite HY.

## تحضير وأداء محفزات الزيوليت HY المعدلة بـ $Mo_2C$ لإصلاح النافثا

### الخلاصة:

تم تطوير محفزات زيوليت HY المعدّلة بـ $Mo_2C$ لتعزيز تفاعلات نزع الهيدروجين والأزمرة في عملية الإصلاح الحفزي للنفثا. وقد تم تحضير نظامين مركبين هما $Mo_2C$–Pt/CeY و Pt–Ti/HY، وتم توصيفهما باستخدام تقنيات حيود الأشعة السينية(XRD) ، ومساحة السطح النوعية(BET) ، والأشعة تحت الحمراء بتحويل فورييه.(FTIR)

تم تقييم الأداء الحفزي في وحدة إصلاح تجريبية عند درجات حرارة تراوحت بين 480–520 °م، وضغوط بين 10–15 بار، وبمعدل سرعة فراغية سائلة (LHSV) مقداره 2 ساعة$^{-1}$، ونسبة هيدروجين إلى هيدروكربون ($H_2$/HC) بلغت 4.

أظهرت النتائج أن إدخال التيتانيوم يحسن التوازن بين المواقع المعدنية والحامضية، ويعزز وظيفة الهدرجة–نزع الهيدروجين من خلال تكوين أنواع تيتانيوم ذات تنسيق رباعي السطوح. ومن بين المحفزات المختبرة، أظهر محفز Pt–Ti/HY أداءً متفوقًا، حيث حقق رقم أوكتان بحثي (RON) بلغ 86.2 ومردودًا من المركبات العطرية بنسبة 27.2% وزنيًا عند درجة حرارة 520 °م وضغط 15 بار.

توضح هذه النتائج أن تعديل زيوليت HY بالمعادن يسهم بشكل كبير في تحسين النشاط الحفزي والانتقائية في عملية الإصلاح الحفزي للنفثا.

# 1. Introduction

Contemporary refineries employ catalytic naphtha reforming units to generate aromatic hydrocarbons, high-octane naphtha, and hydrogen, accounting for 40% of global production. The catalytic reforming of naphtha enhances the octane rating of the feedstock, rendering it suitable for gasoline formulations [1, 2]. This octane rating assesses gasoline's ability to prevent knocking and its environmental impact. Additional characteristics are vital for optimal functionality. [3, 4] Catalytic naphtha reforming transforms low-octane compounds into high-octane gasoline while preserving carbon chain lengths. This process converts straight-chain naphtha into iso-paraffins and aromatics, or generates substantial quantities of benzene, toluene, and xylenes for petrochemical feedstocks. Hydrogen is crucial for hydrocracking and hydrotreating processes in refineries. Long-chain hydrocarbons experience isomerization, hydrogenation, dehydrocyclization, and dehydrogenation reactions on acidic and metallic sites during rapid catalytic reforming. Bifunctional catalysts operate on solid supports such as chlorinated alumina and noble metals. These reactions enhance dehydrocyclization and other processes, while simultaneously promote hydrogenolysis and hydrocracking, which diminish valuable products and deactivate the catalyst by producing coke on active sites. This article addresses the selection of support materials for carbides to mitigate Cl leaching [6]. Solid acid supports, such as titanium oxide-promoted zeolite, being investigated as non-chlorinated substitutes for alumina. A transition metal carbide with platinum on HY zeolite catalyzes the reforming of heavy naphtha in a packed bed reactor. In the identical pilot plant, a comparison is made between HY zeolite with Pt–Ti loading and modified Y with transition metal carbide and Pt. [7]

## 1.1. Carbide catalyst

Carbides are categorized into three types: interstitial, intermediate, and salinic. Interstitial chemicals are susceptible to water damage and exhibit instability at low temperatures. Transition metal carbides have intricate chemical bonds, encompassing ionic, covalent, and metallic interactions. These compounds have elevated hardness and melting points, defined by ionic, covalent, or metallic bonding. The electrical structure of transition metal carbides is thoroughly studied, with covalent bonding being the primary feature. Carbides are utilized in industry for applications such as strength-enhancing materials, ceramics, protective coatings, and the refinement of cutting tool blades. They are utilized in catalytic processes, including hydrotreatment, hydrodesulfurization, hydrodenitrogenation, and hydrodeoxygenation. Molybdenum carbides are characterized by a melting point exceeding 2,000°C, exceptional thermal stability, high conductivity, corrosion resistance, and significant hardness. They are utilized in cutting tool components, electrocatalysis, anti-creeping alloys, and catalysis. [8,9]

Platinum (Pt) is a pricey industrial catalyst due to its efficacy and endurance. It makes up roughly 90% of the catalyst's cost. To solve this, researchers are investigating other metals and materials with similar activity and stability. Transition metal carbides (TMC) have high melting points, excellent electrical properties, and better thermal stability. Due to their Fermi level electronic states, these materials behave like platinum group metals.

Metal-catalyzed naphtha reforming uses TMC catalysts like tungsten and molybdenum carbides for isomerization and dehydrogenation. The lack of support in these materials may explain their catalytic action. Levy and Boudart found that Pt, Ir, and Au may isomerize 2,2-dimethylpropane to 2-methylbutane, informing carbide catalyst research.

Dye-sensitized solar cells using molybdenum carbide counter electrodes convert energy more efficiently than platinum. This method has also decomposed hydrazine and converted cellulose into polyols like ethylene glycol.

Molybdenum carbide's catalytic selectivity is another feature. Unique catalytic pathways favor product selectivity. The Mo2C/AC catalyst, which contains nanoscale active carbon, may transform renewable oils into diesel-like hydrocarbon mixtures. As a catalyst for vegetable oil hydrodeoxygenation, molybdenum carbide shows selectivity and activity. [10, 11, 12]

This study aims to develop and evaluate non-chlorinated zeolite-based bifunctional catalysts (Pt–Ti/HY and $Mo_2C$–Pt/CeY) for naphtha catalytic reforming. It focuses on improving catalytic activity, aromatics selectivity, and stability while reducing coke formation and eliminating chlorine-related drawbacks under industrial operating conditions.

## 2. Experimental work:

### 2.1. Feed Stock:

Heavy Naphtha supplied by the North Refineries Company/ Baiji as raw material for the reforming activity test was used. Some properties of heavy Naphtha given by the supplier are listed in Table (1). All the materials used to prepare the catalysts are shown in Table (2).

**Table (1):** Properties of Heavy Naphtha

| | |
|---|---|
| Sulfur content, ppm | 0.1 |
| Density, g/ $cm^3$ | 0.73 |
| Paraffins, wt.% | 61.3 |
| Aromatics, wt.% | 13 |
| Naphthenes wt.% | 25.7 |
| I.B.P ºC | 40 |
| E.B.P ºC | 270 |
| RON | 57 |

**Table (2):** Chemical used in the study. [8]

| Chemicals | Formula % | Molecular weight g/mol | Purity | Supplier |
|---|---|---|---|---|
| **Activated carbon** | C | 14 | 100 | |
| **HY-zeolite*** | $Na_2O:Al_2O_3:SiO_2:H_2O$ | | | |
| **Ammonium Molybdate tetrahydrate** | $(NH4)6Mo_7O_{24}.4H_2O$ | 115.03 | 99 | ROMIL |
| **Hexachloroplatinic acid** | $H2PtCl_6.6H_2O$ | 517.92 | 40 | REIDL |
| **Cerium nitrate** | $CeN_3O_9.6H_2O$ | 434.22 | 99 | SIGMA - ALDRICH |

### 2.2. Preparation of ($Mo_2C$-Pt/CeY) Molybdenum carbide zeolite composite catalyst

Solid-state synthesis was used to create molybdenum carbide supported on activated carbon. Activated carbon was added to a metal salt solution and agitated for two hours, and then the solvent evaporated and dried in a 150°C oven for 4 hours. The carbide materials were heated at 900° C and cooled to room temperature after the reaction.

The zeolite HY powder was modified using ion exchange with nitrate solutions of cerium cation $Ce(NO_3)_3$. The sample was exchanged at 80°C for 8 hours, filtered, washed, dried at 120°C, and calcined at 600°C for 5 hours to produce a Ce-modified Zeolite Y. The final Platinum catalyst containing (carbide and HY as a carrier) is prepared via the impregnation method using hexachloroplatinic acid; then the sample is washed, filtered, and dried at 120° C before entering a furnace at 600°C for 6 hours, as in Figure (1). [8]

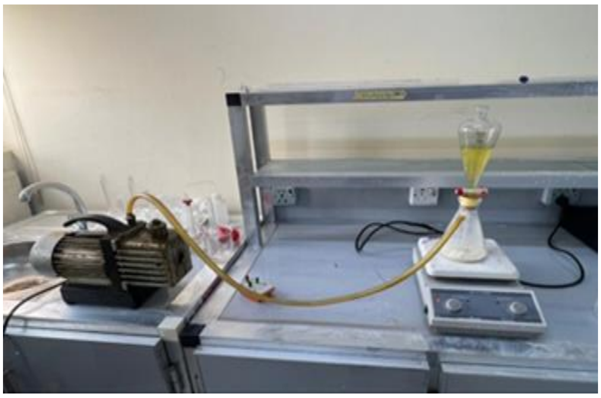

**Fig. (1):** Preparation of Metal loaded catalyst

### 2.3. Preparation of (Pt -Ti / HY) Platinum promoted by Titanium ion exchanged by cerium Y zeolite catalyst

The zeolite HY powder was modified. The final (Pt- Ti) loaded catalyst of Ce-modified Zeolite Y is prepared via the impregnation method using hexachloroplatinic acid and titanium butoxide. Then, the sample is washed, filtered, and dried at 120°C before entering a furnace at 600°C for 6 hours. [9]

## 3. Results and Discussion

### 3.1. BET surface area and pore volume analysis:

BET surface area and pore volume were analyzed for all catalysts to evaluate it. The physical and chemical properties of prepared catalysts are tabulated in Table (3).

The synthesized $Mo_2C$.Pt/CeY catalyst has a 718.113 $m^2/g$ BET surface area, while PtTi /HY is 575 $m^2/g$, resulting in macroporous and mesoporous particles, increasing pore volume and potential for heavy naphtha reforming.

**Table (3):** Physical Properties of Prepared Catalyst

| Catalysts | Surface area $m^2/g$ | Pore volume $cm^3/g$ |
|---|---|---|
| Pt.Ti/HY zeolite | 575 | 0.38 |
| $Mo_2C$.Pt/CeY zeolite | 718.1 | 0.75 |

### 3.2. Fourier transform

Both catalysts retain the zeolite structure, confirmed by the strong ~1060 $cm^{-1}$ band, though slight shifts in $Mo_2C$–Pt/CeY indicate framework interaction with Ce and Mo species.

- Acidity Differences: The Pt–Ti/HY catalyst shows stronger Brønsted acidity (~940 $cm^{-1}$), which favors isomerization reactions. In contrast, acidity is partially modified in $Mo_2C$–

Pt/CeY due to cerium exchange.

- Metal Incorporation: The $Mo_2C$–Pt/CeY catalyst exhibits stronger low-frequency bands (500–550 $cm^{-1}$), confirming better metal–support interaction compared to Pt–Ti/HY.
- Hydrocarbon Interaction: The more intense ~1550 $cm^{-1}$ band in $Mo_2C$–Pt/CeY suggests stronger adsorption or formation of aromatic intermediates as listed in Table 4. And showed in Figure (3).

Pt–Ti/HY exhibits stronger acidity and balanced metal–acid functionality, while $Mo_2C$–Pt/CeY shows enhanced metal–support interaction and hydrocarbon activation. This explains the superior reforming performance of Pt–Ti/HY in terms of octane number and selectivity.

**Table (4):** Comparsion between functional groups of prepared catalysts

| **Wavenumber ($cm^{-1}$)** | **Pt–Ti/HY Zeolite** | **$Mo_2C$–Pt/CeY Zeolite** | **Interpretation** |
|---|---|---|---|
| **~2345** | Weak $CO_2$ adsorption | Weak $CO_2$ adsorption | Atmospheric $CO_2$ (common in both). |
| **~1635** | Moderate | Moderate–strong | Adsorbed water; slightly higher in CeY due to higher polarity. |
| **~1550–1560** | Present | More pronounced | Aromatic C=C or hydrocarbon species; enhanced in $Mo_2C$ system. |
| **~1060** | Strong | Strong (slightly shifted) | Si–O–Si framework; slight shift indicates structural modification. |
| **~940–950** | Clear band | Reduced intensity | Brønsted acid sites; partially modified by Ce and $Mo_2C$. |
| **~700** | Moderate | Moderate | Framework vibration (both stable) |
| **~530–550** | Weak (Ti–O) | Stronger (Mo–O / Ce–O) | Metal–oxygen bonding; stronger in $Mo_2C$–Pt/CeY. |
| **~450** | Weak | Weak | T–O bending (framework integrity). |

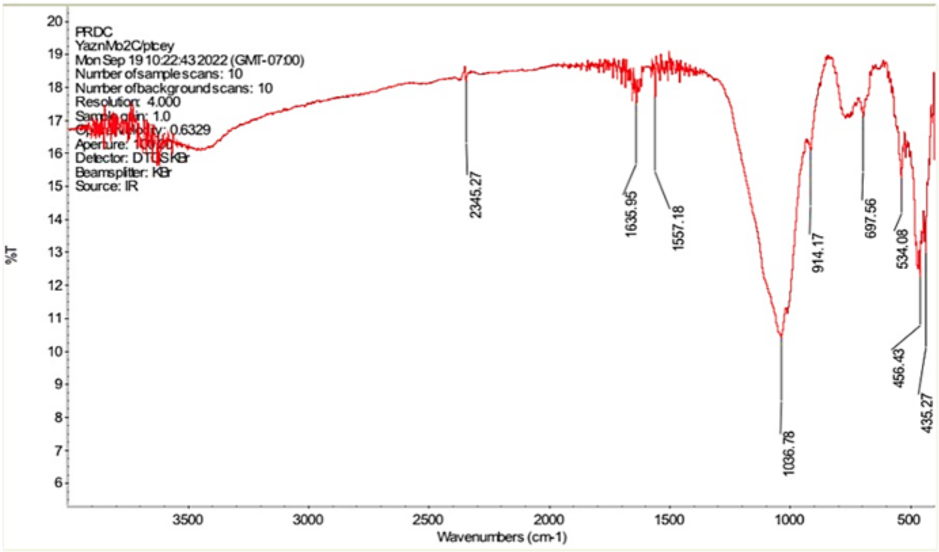

**Fig. (3):** FTIR for $Mo_2C$.Pt/CeY zeolite catalyst

### 3.3. X-ray diffraction of final prepared catalyst

The X-ray diffraction (XRD) patterns illustrated in Figure (4) (Pt–$MoO_2$–Ce/Y zeolite) and Figure (5) (Pt–Ti/HY zeolite) exhibit notable variations in crystallographic structure, phase distribution, and crystallinity, which are directly associated with catalyst composition and metal–support interactions. Figure (4) displays a diffraction pattern characterized by a series of moderately sharp peaks overlaid on a broad diffuse background across the range of approximately 10–35° (2θ), signifying the presence of crystalline phases with a substantial amorphous component. The distinctive reflections noted at around 22°, 26–30°, and 42–45° are ascribed to the Y-zeolite structure, supplemented by contributions from distributed $MoO_2$ and cerium-containing oxide species. The evident peak broadening indicates diminished crystallite size and/or lattice distortion, commonly linked to robust metal–support interactions and elevated dispersion of active species within the zeolite matrix. These structural characteristics are frequently advantageous for catalytic applications because they boost the accessibility of active sites and augment surface area.

Figure (5) for Pt–Ti/HY zeolite has a distinctly crystalline diffraction pattern marked by strong, powerful, and well-defined peaks throughout the full 2θ range (10–60°). The existence of several reflections, especially in the ranges of around 15–35° and 40–60°, signifies a well-preserved HY zeolite framework alongside supplementary crystalline phases linked to Ti-containing species and supported platinum. The markedly reduced peak widths (decreased full width at half maximum, FWHM) relative to Figure (4) indicate larger crystallite dimensions and enhanced long-range structural order. The concordance between experimental peaks and reference stick patterns verifies the establishment of a multiphase crystalline system characterized by enhanced structural stability and diminished amorphous content.

A direct comparison of the 2θ band distribution reveals that the low-angle area (10–20°) in Figure (4) exhibits well-defined reflections, while Figure (4) displays only weak and widened patterns, signifying a greater degree of structural disorder in Pt–$MoO_2$–Ce/Y zeolite. In the mid-angle area (20–35°), Figure (4) features fewer and larger peaks, but Figure (5) displays many sharp reflections associated with specific crystallographic planes, indicating enhanced phase segregation and crystallinity in the Pt–Ti/HY system. In the high-angle area (35–60°), the sparse and feeble reflections in Figure (4) stand in stark contrast to the abundant, well-defined peaks in Figure (4), so further validating the enhanced crystallographic order of the latter.

The structural differences between the two catalysts can be elucidated through synthesis and compositional impacts. The introduction of Ce and Mo species in Figure (4) likely generates lattice strain and partial amorphization due to defect formation and robust interaction with the zeolite framework. In contrast, the incorporation of Ti species into HY zeolite Figure (5) seems to enhance the stability of the crystalline framework and facilitate the development of well-defined phases. These structural changes are anticipated to affect catalytic performance, with Pt–$MoO_2$–Ce/Y potentially demonstrating superior dispersion and activity, while Pt–Ti/HY may provide improved thermal stability and structural integrity. [7],[9].

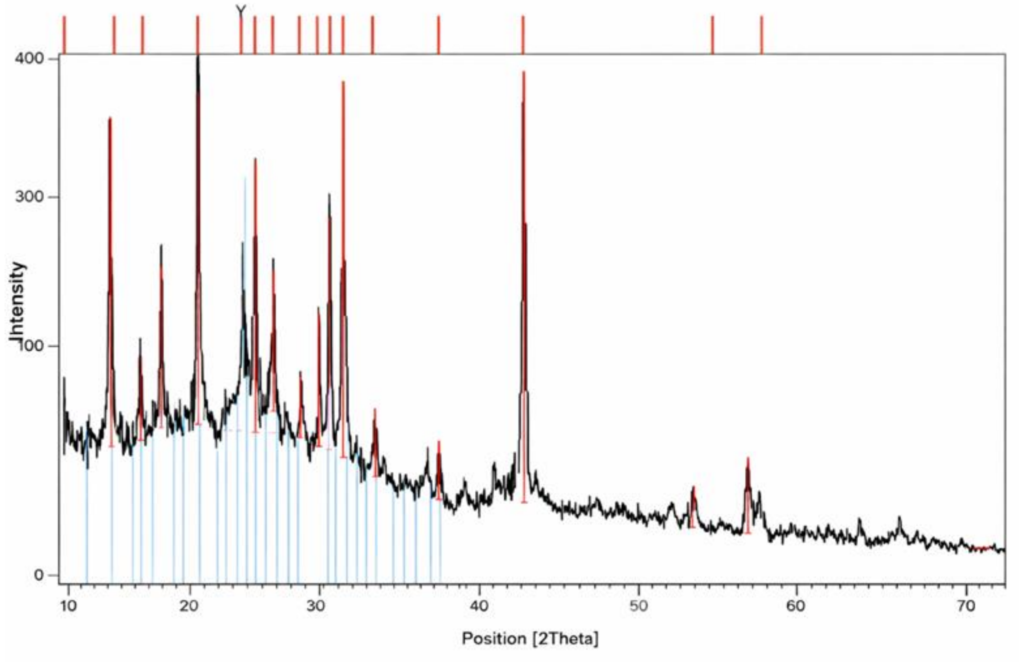

**Fig. (4):** X-Ray diffraction patterns of prepared $Mo_2C$.Pt/CeY zeolite catalyst

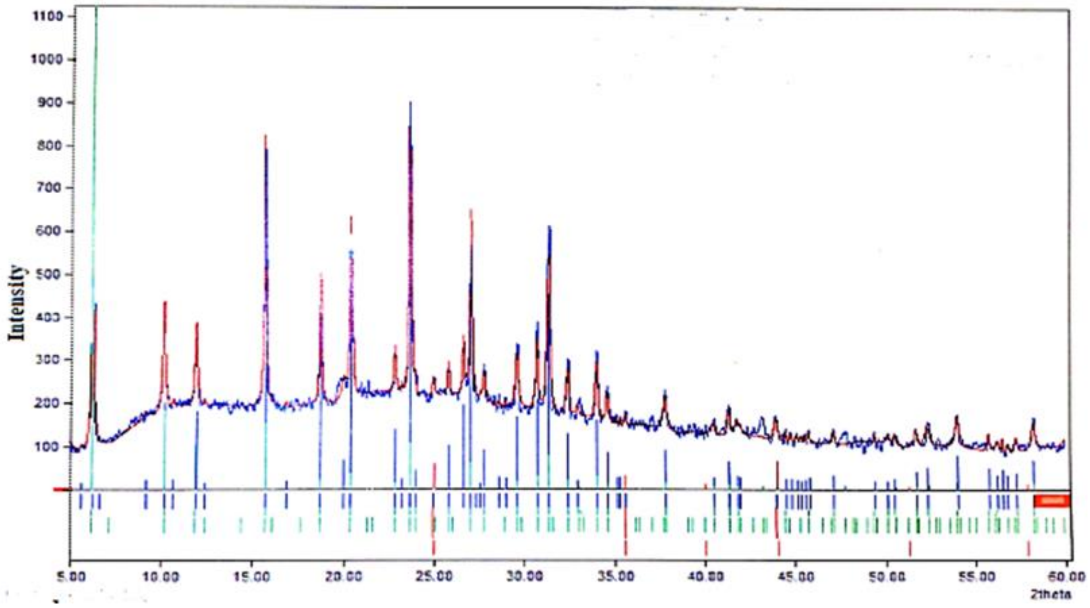

**Fig. (5):** X-Ray diffraction patterns of prepared Pt-Ti /HY zeolite catalyst

### 3.4. Activity testing

The study examines naphtha catalytic reforming on three catalyst samples to produce high-octane reformate. The study uses a fixed bed reactor with two layers of inert ceramic spheres. The reactor's operation conditions include reaction temperatures (480, 500, and 520 °C), pressure (10, 12.5, and 15 bar), and constant LHSV and mole ratio ($2h^{-1}$ and $H_2/H_C=4$). PONA analysis is conducted for the product.

The study investigates the impact of reaction temperatures on heavy naphtha catalytic reforming efficiency. The reaction temperature is a crucial operational parameter affecting the octane rating of the reformate. Increased reaction pressure leads to increased hydrocracking reactions, resulting in a decrease in product reformate but an increase in catalyst coking. Decreased reaction pressure also increases Naphthenes' dehydrogenation and paraffin's hydrocyclization, causing an increase in catalyst coking. Hydrocracking may increase octane by converting large molecules like n-decane to C3 and C7 into aromatic materials. Although unfavorable, it can prolong the life of carbonaceous materials.[1],[5].

The aromatics product increases due to isomerization reactions, while the percentages of paraffin and naphthenic groups decrease.

The $Mo_2C$.Pt/CeY zeolite catalyst's performance at different reforming temperatures (480, 500, and 520°C) and pressures (10, 12.5, 15 bar) is shown in Figures (4) to (7). The temperature change does not significantly impact product weight percent, but 500°C results in higher octane numbers due to aromatics and naphthenes.[8][13].[14].

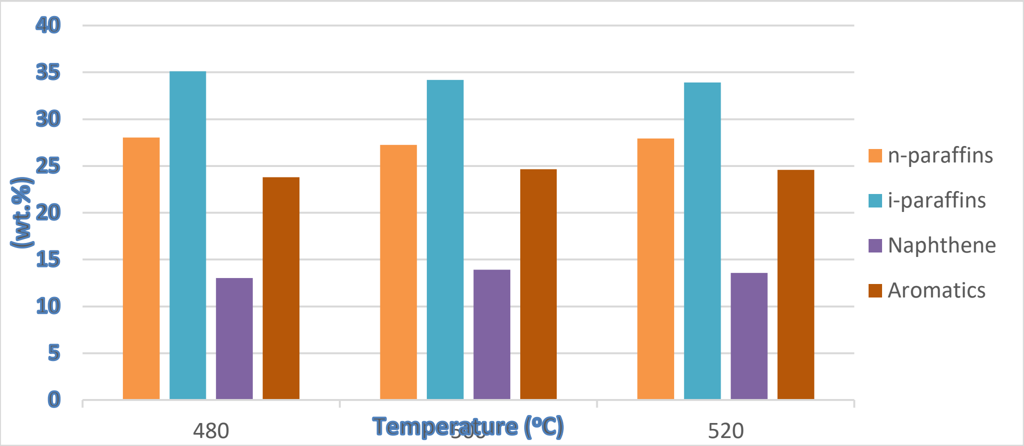

**Fig. (4):** Product distribution for ($Mo_2C$.Pt/CeY zeolite) catalyst at a pressure of 10 bar at different reaction temperature

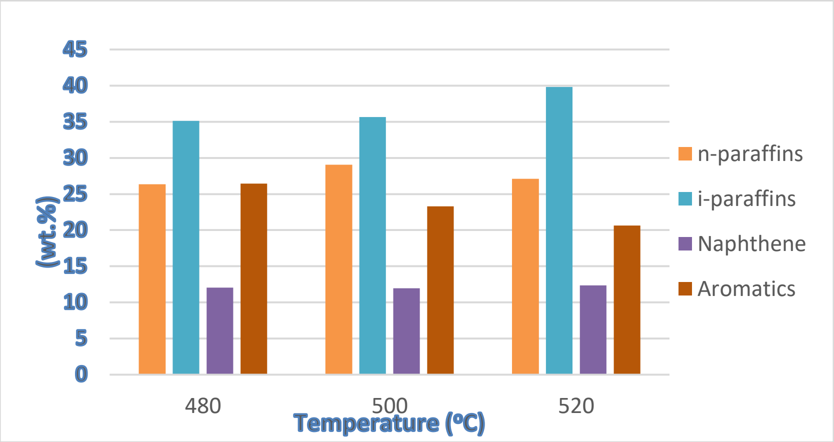

**Fig. (5):** Product distribution for ($Mo_2C$.Pt/CeY zeolite) catalyst at a pressure of 12.5 bar at different reaction temperatures

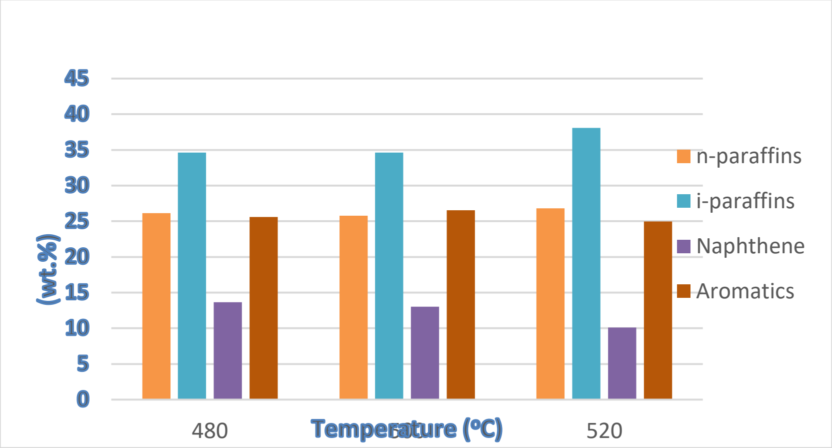

**Fig. (6):** Product distribution for ($Mo_2C$.Pt/CeY zeolite) catalyst at a pressure of 15 bar at different reaction temperature

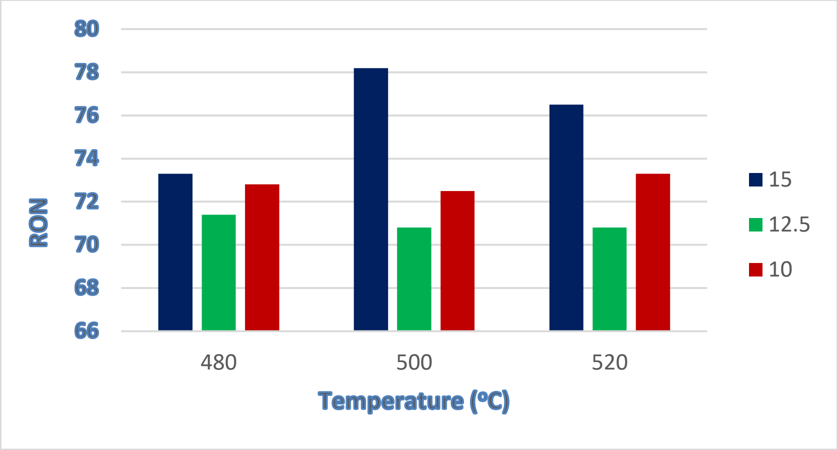

**Fig. (7):** Research Octane Number for ($Mo_2C$.Pt/CeY zeolite) at different temperature and pressure

The Pt. Ti/HY zeolite catalyst performs better than Mo2C.Pt/HY and Mo2C.Pt/CeY zeolite in various reforming temperatures. It has a higher aromatics yield, leading to higher octane numbers. The best results were obtained at 500°C, as increasing temperature causes unfavorable hydrocracking processes, lowering the octane number of the reformate. The composite catalyst's bimetallic loading is related to combining titanium and platinum to create an alloy that keeps platinum well-dispersed, prevents sintering, and prevents coke precursors from adhering to catalyst surfaces, as indicated in Figures. (8) to (11).[8],[11][15].

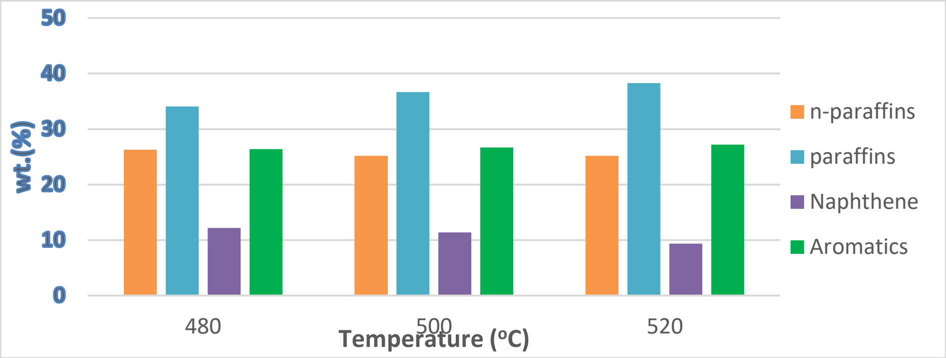

**Fig. (8):** Product distribution for (Pt. Ti/HY zeolite) catalyst at a pressure of 10 bar at different reaction temperatures

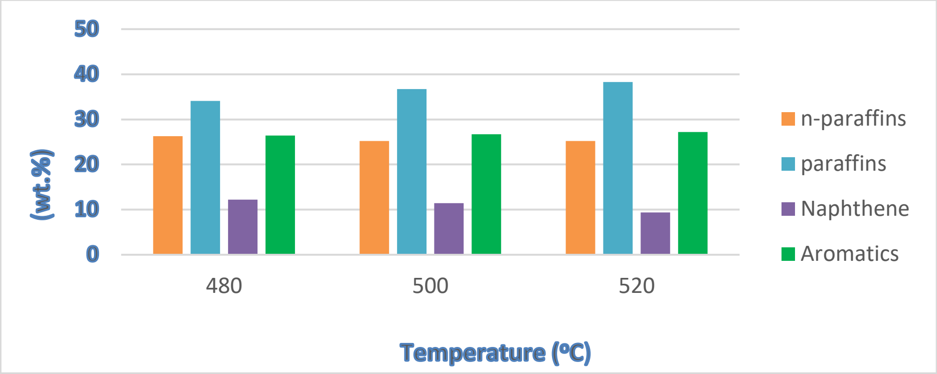

**Fig. (9):** Product distribution for (Pt. Ti/HY zeolite) catalyst at a pressure of 12.5 bar at different reaction temperatures

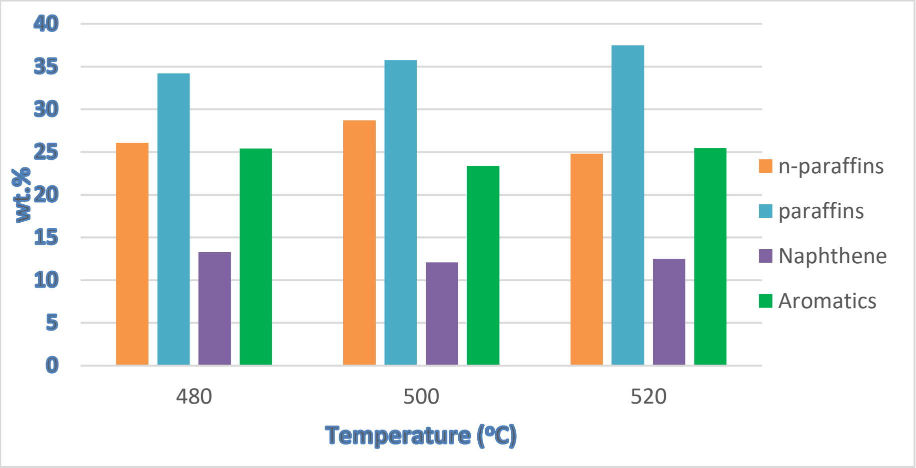

**Fig. (10):** Product distribution for (Pt. Ti/HY zeolite) catalyst at a pressure of 15 bar at different reaction temperatures

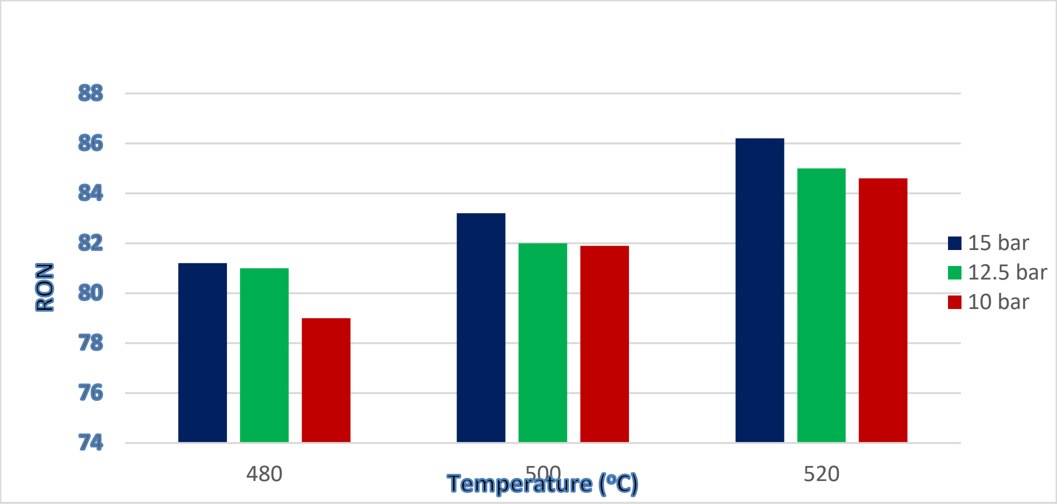

**Fig. (11):** Research Octane Number for (Pt Ti / HY zeolite) at different temperature and pressure

Increases in rates, activity, and aromatic yield are indicative of greater selectivity, and the activity of a catalyst is a reflection of how effectively it performs its role. It is possible that the incorporation of metal has an effect on the acidic characteristics of the support, which in turn has an effect on the activity and selectivity of the catalysts that are produced. Within the framework of the catalytic naphtha reforming process, bifunctional reactions take place on acidic HY zeolite and metallic sites such as Pt, MoC, and Ti. In catalytic reforming, the yield of the reformate is extremely important because an increase in quality results in a decrease in yield and vice versa. A further key criterion is the octane rating, which is used to evaluate the quality of the reformate product. Mo2C.Pt/CeY zeolite comes in second place after Pt.Ti/HY zeolite's octane number, which is the highest of any zeolite.

The octane number, which measures the quality of the product reformate, is another crucial criterion. Pt.Ti/HY zeolite has the best octan number, followed by Mo2C.Pt/CeY zeolite.[8],[9][14],[15].

## 4. Conclusions

The Naphtha reforming reaction was investigated using prepared catalysts, showing good activity, stability, and selectivity. The maximum RON obtained was 86.2 for Pt Ti / HY catalyst and 78.2 for Mo2C Pt / CeY zeolite.

Titanium incorporation improves Pt/HY catalyst catalytic activity for Naphtha reforming reactions through dehydrogenation-hydrogenation reactions.

- Both catalysts show similar general trends with temperature, but **selectivity differs significantly**.

- Carbide Catalyst **Mo2C Pt/ CeY** promotes **branched paraffins (iso-paraffins)**, indicating strong isomerization activity.
- Acid Catalyst **Pt Ti /HY** enhances **aromatic formation**, indicating stronger dehydrogenation and cyclization activity.
- The choice of catalyst depends on the desired product:
  - **Cleaner fuels → Carbide Catalyst.**
  - **High-octane reformate → Acid Catalyst.**

**Author Contributions Statement:** Ban A. Altabbakh contributed to the Conception; Methodology; Data Analysis and Interpretation; Writing – Original Draft; Writing – Review & Editing, Aysar T. Jarullah contributed to the Conception; Methodology; Data Analysis and Interpretation, Writing – Original Draft; Writing – Review & Editing. Ahmed N. Ahmed contributed to the Investigation/ Experiments; Data Curation and Analysis; Writing – Original Draft; Writing – Review & Editing. All authors have read and approved the final version of the manuscript.

## References

[1] C. L. Pieck, C. R. Vera, J. M. Parera, G. N. Giménez, L. R. Serra, L. S Carvalho, and M. C. Rangel, "Metal dispersion and catalytic activity of trimetallic Pt-Re-Sn/$Al_2O_3$ naphtha reforming catalysts", *Catalysis Today*, vol. 107-108, pp. 637–642, 2005. https://doi.org/10.1016/j.cattod.2005.07.040.

[2] S. A. D'Ippolito, C. R. Vera, F. Epron, C. Especel, P. Marécot, and C. L. Pieck, "Naphtha reforming Pt-Re-Ge/$\gamma$-$Al_2O_3$ catalysts prepared by catalytic reduction: Influence of the pH of the Ge addition step", *Catalysis Today*, vol. 133, pp. 13–19, 2008. https://doi.org/10.1016/j.cattod.2007.11.014.

[3] G. J. Antos and A. M. Aitani, "Catalytic naphtha reforming, revised and expanded", *CRC Press*, 2004.

[4] T. Lid and S. Skogestad, "Data reconciliation and optimal operation of a catalytic naphtha reformer", *Journal of Process Control*, vol. 18, no. 3–4, pp. 320–331, 2008. https://doi.org/10.1016/j.jprocont.2007.09.002.

[5] N. S. Ahmedzeki, B. A. Al-tabbakh, M. B. Antwan, S. Ylemiz, "Heavy naphtha upgrading by catalytic reforming over novel bi-functional zeolite catalyst", *Reaction Kinetics, Mechanisms and Catalysis*, vol.125, pp. 1127-1138, 2018. https://doi.org/10.1007/s11144-018-1432-y.

[6] R. A. Meyers, "Handbook of petroleum refining processes", *McGraw-Hill Education*, 2016.

[7] A. T. Jarullha, A. N. Ahmed, B. A. Al-tabbakh, and A. M. Ahmed, "Design of New Composite Nano-Catalyst for Naphtha Reforming Process: Experiments and Process Modeling", *Tikrit Journal of Engineering Sciences*, vol.30, no. 2, pp. 46-59, 2023. https://doi.org/10.25130/tjes.30.2.6.

[8] J. L. Hodala, S. Kotni, B. Ramachandrarao, and B. Chelliahn, "Metal carbide as a potential non-noble metal catalyst for naphtha reforming", *Fuel*, vol. 288, p. 19610, 2021. https://doi.org/10.1016/j.fuel.2020.119610.

[9] N. S. Ahmedzeki and B. A. Al-Tabbakh, "Catalytic reforming of Iraqi Naphtha over Pt-Ti/HY zeolite catalyst", *Iraqi Journal of Chemical and Petroleum Engineering*, vol. 17, no. 3, pp. 45–56, 2016. https://doi.org/10.31699/IJCPE.2016.3.4.

[10] S. R. S. Mohaddecy, S. Zahedi, S. Sadighi, and H. Bonyad, "Reactor modeling and simulation of catalytic reforming process", *Petroleum & Coal*, vol. 48, no. 3, pp. 28–35, 2006.

[11] U. Taskar and J. B. Riggs, "Modeling and optimization of a semiregenerative catalytic naphtha reformer," AIChE Journal, vol. 43, no. 3, pp. 740–753, 1997. https://doi.org/10.1002/aic.690430319.

[12] L. B. Galperin, J. C. Bricker, and J. R. Holmgren, "Effect of support acid–basic properties on activity and selectivity of Pt catalysts in the reaction of methylcyclopentane ring opening", *Applied Catalysis A: General*, vol. 239, no. 1–2, pp. 297–304, 2003. https://doi.org/10.1016/S0926-860X(02)00416-7.

[13] C. Gao, D. Li, H. Pan, H. Wang, Y. Zhu, Y. Tang, M. Zhu, Z. Yang, and J. Xu, “Propane-Induced Pt/Al2O3 Surface Reconstruction for Catalytic Reforming Reaction of n-Heptane”, *ACS Catalysis*, vol. 15, no. 22, pp. 18953-18965, 2025. https://doi.org/10.1021/acscatal.5c05811.

[14] F. Velázquez-Alonso, C. A. González-Ramírez, J. R. Villagómez-Ibarra, E. M. Otazo-Sánchez, M. Hernández-Juárez, F. Pérez-Villaseñor, A. Castro-Agüero, and L. O. Alemán-Vázquez, “Transitional analysis for multi-objective operative improvement of reformate quality and hydrogen production from a naphtha catalytic reforming process”, *Heliyon*, vol. 11, no. 1, 2025. https://doi.org/10.1016/j.heliyon.2024.e41428.

[15] F. Velázquez-Alonso, C. A. González-Ramírez, J. R. Villagómez-Ibarra, E. M. Otazo-Sánchez, M. Hernández-Juárez, F. Pérez-Villaseñor, Á. Castro-Agüero, Á. Castro-Agüero, L. O. Alemán-Vázquez, C. Camacho-López, and C. Romo-Gómez, “Operative Improvement in the Naphtha Catalytic Reforming Process to Reduce the Environmental Impact of Benzene Fugitive Emissions from Gasoline”, *ChemEngineering*, vol. 9, no. 2, p. 21, 2025. https://doi.org/10.3390/chemengineering9020021.